Green synthesis of silver nanoparticles using *gesho* (*Rhamnus prinioides*) fruit extract and evaluation of their antibacterial activity

Muluken Aklilu Solomon*

Department of Chemistry, Bahir Dar University, Bahir Dar, Ethiopia.

Received: November 15, 2022 **Accepted:** April 21, 2023 **Published:** June 30, 2023

ABSTRACT

Nowadays, the applications of metal nanoparticles are growing rapidly in different fields due to their unique properties such as size and shape. Among these nanomaterials, silver nanoparticles (Ag NPs) are commonly used in many applications due to their unique optical properties, relatively high stability, and strong conjugation ability with biomolecules. Several eco-friendly approaches have been used to synthesize the nanoparticles. Many scientists are focused on green synthesis of nanoparticles from plant extracts. In the context of this, we have investigated the fruit of *Rhamnus prinoides* L'Herit to make innumerable sources of cost-effective, non-hazardous reducing and stabilizing compounds utilized in preparing Ag NPs. During the synthesis of the nanoparticle, we used 5% (w/v) of 50 mL *R. prinoides* fruit extract and 3 mM of 50 mL silver nitrate solution. The formation and characterization of Ag NPs were confirmed by UV-Vis spectrophotometry, XRD and FTIR methods. Thus, the formation of a deep red colored solution and the UV-visible absorption peak at 416 nm was taken as an initial confirmation of Ag NPs formation. The result was due to the excitation of the surface plasmon resonance in the Ag NPs. While the FTIR spectroscopic study showed the involvement of *R. prinoides* fruit extract in the reduction of Ag^+ ions to Ag NPs. The particle size of the synthesized nanoparticles, in accordance with XRD result, was calculated using Debye Sherrer's equation and the result was found to be equal to 21 nm. The antibacterial activity of the silver nanoparticles against pathogenic microorganism strains of *Escherichia coli* and *Staphylococcus aureus* was confirmed by the disc diffusion method and was found to inhibit the growth of the bacteria with an average zone of inhibition size of 23 mm against *E. coli* and 13 mm against *S. aureus*. The results showed that green synthesized Ag NPs exhibited significant antimicrobial potency.

Keywords*:* Silver Nanoparticles; Green synthesis; *Rhamnus prinoides*; Fruit extract; Antibacterial activity

DOI: https://dx.doi.org/10.4314/ejst.v16i2.2

INTRODUCTION

Nanoparticles represent a particle with a nanometer size of 1–100 nm. The nanoscale material has new, unique, and superior physical and chemical properties compared to its bulk structure, due to an increase in the ratio of the surface area per volume of the material/particle (Aritonang *et al.,* 2019*;* Rautela *et al.,* 2019). Nanoparticles exhibit enhanced properties on specific characteristics such as size, shape, composition, distribution, crystallinity and morphology (Siddiqi *et al.,* 2018). Among the different

* Corresponding author: mulukenak@gmail.com

nanomaterials developed so far, nanomaterials of novel metals in particular Ag, Pt, Au and Pd have established their potentiality in many fields due to their various unique properties like catalysis, high electrical conductivity, chemical stability, optoelectronics, display devices, diagnostic biological probes, anti-microbial activity etc (Aritonang *et al.,* 2019*;* Pirtarighat *et al.,* 2019; *Vanlalveni et al.,* 2021). In this context, particularly Ag nanoparticles are well known for potential applications in the field of medicine technology including drug delivery, antimicrobial efficacy against bacteria, viruses and other eukaryotic microorganisms, etc. (Shaik *et al.,* 2018; Hemlata *et al.,* 2020). Research activity that has already been carried out on Ag nanoparticles reveals that they possess high antibacterial activity against Gram-negative as well as Gram-positive bacteria and antiviral activity against HIV-1 virus, respiratory syncytial virus, hepatitis B virus, etc. (Malik *et al.,* 2022).

Over the years, several routes such as conventional chemical reduction, electrochemical reduction, photochemical reduction, etc. and most recently biological green routes have been developed to synthesis Ag nanoparticles in a wide range of particle size (Giri *et al.,* 2022).

After detail review of current literature on biosynthesis of nanoparticles using green chemistry, it may be concluded that the extracts of various plant parts are frequently used for synthesis of Ag nanoparticles due to the presence of reducing and stabilizing agents within their extracts (Elhawary *et al.,* 2020; Arroyo *et al.,* 2021). Furthermore, the use of extracts of different parts of plants cuts down the level of cost of the synthesis and does not require elaborate processes such as intracellular synthesis and multiple purification steps or the maintenance of microbial cell cultures (Jain and Mehata, *2*017*;* Ndikau *et al.,* 2017*;* Moond *et al.,* 2022). The need for environmental nontoxic synthetic protocols for nanoparticles synthesis leads to the developing interest in biological approaches which are free from the use of toxic chemicals as byproducts. Thus, there is an increasing demand for "green nanotechnology." Many green synthesis approaches for both extracellular and intracellular nanoparticles synthesis have been reported till date using microorganisms including bacteria, fungi, and plants (Masum *et al.,* 2019).

Based on the previous literature reports, Ag nanoparticles have been synthesized from extracts of various plant parts such as fruit extracts of *Momordica cymbalaria* (Hemalatha *et al.,* 2021), *Citrus tangerina*, *Citrus sinensis*, and *Citrus limon* (Niluxsshun *et al.,* 2021), *Diospyros malabarica* (Bharadwaj *et al.,* 2021), clammy cherry (*Cordia obliqua* Willd) (Saidu *et al.,* 2019), *Aegle marmelos* (Devi *et al.,* 2020), *Cleome viscosa* L. (Lakshmanan *et al.,* 2018), etc. In this concern, Ethiopian flora has yet to make innumerable sources of cost-effective non-hazardous reducing and stabilizing compounds utilized in preparing Ag NPs. Fig. 1 shows the mechanism of reduction of silver ions to Ag NPs by a phytochemical called quercetin molecule

obtained from plant extracts (Jain and Mehata, 2017).

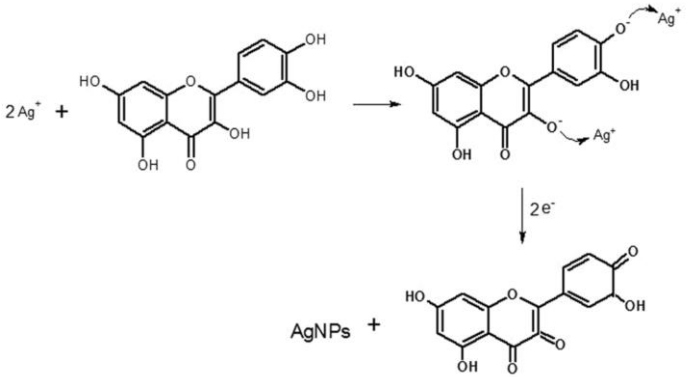

Figure 1. Mechanism of reduction of silver ions to Ag NPs by quercetin molecule

In this study, we have reported to the best of our knowledge for the first time, the synthesis of Ag nanoparticles by reducing silver ions in the presence of fruit extract of *R. prinoides* (Figure 2)**.** *R. prinoides*, commonly called *'*Gesho*'* in Ethiopia, is an endemic plant to Ethiopia which grows to a height of about six meters, ecologically widespread, and locally cultivated from medium to high altitudes (1000-3200 m)**.** It has high social and economic importance in many rural and urban communities of the country (Habtemariam and Alemu, 2022; Eyob, 2017).

Figure 2. Picture of *Rhamnus prinoides* fruit

In Ethiopia, the fruit of *R. prinoides* is used for consumption mainly as an additive in brewing local beverages, i.e., traditional homemade alcoholic drinks including *tella*, *katikala* and *tej* (Eyob, 2017). The leaves and stems of *R. prinoides* are used to impart the characteristic bitter taste to traditional fermented beverages, such as *tella* and *tej*. The plant has been reported to regulate the microflora responsible for the fermentation

process. It plays an important role in suppressing certain bacteria during the fermentation process. The fruits of this plant are used for ringworm infection treatment (Negash *et al.,* 2021). Moreover, it has traditional medical values to relieve pain and as perennial crop ground cover, is important for soil protection against wind and water erosion (Eyob, 2017*;* Negash *et al.,* 2021). For this work the fruit extract of *R. prinoides* was used due to its ease of availability, low cost and medicinal property.

MATERIALS AND METHODS

Chemicals such as 98% Silver nitrate, 98% Sodium Hydroxide and 25% Ammonia solution (Blulux Laboratories Pvt. Ltd), 99% Ferric chloride, 35.4% Hydrochloric acid and 98% Sulphuric acid (Loba Chemie Pvt. Ltd, India), 99.5 % Ethanol (Unichem Chemicals Pvt. Ltd, India), Gentamicin (Uvasol, Germany), Nutrient Broth and Agar Hilten Muller (Imtech, Chandigarh, India), 99.9% Chloroform (Fisher Scientific UK Ltd), Meyer's reagent, Benedict's solution, 80% Iodine solution and 99% Potassium Iodide (Abron chemicals limited, India), 99.5% Glacial Acetic Acid and 64.7 % Lead acetate (Wagtech International Ltd., UK) and 60% Nitric acid (Lammark chemicals Pvt., India) were used in the experiment. All the chemicals used were analytical grade. Freshly prepared double-distilled water was used throughout the experiment.

Preparation of aqueous solution fruit extract of *Rhamnus prinoides*

R. prinoides fruits were purchased from a local market in Bahir Dar, Ethiopia. To eliminate dirt and other polluted organic substances, the leaves were thoroughly washed first with running tap water and then with distilled water. A beaker containing 20 g of finely crushed *R. prinoides* fruits was filled with 200 mL double distilled water and heated for 30 minutes. To remove particle debris, the extract was cooled down and filtered with Whatman No.1 filter paper. The solutions were then kept at 4 °C until needed. Sterile conditions were maintained throughout the experiment to ensure the effectiveness and correctness of the results.

Synthesis of silver nanoparticles (Ag NPs)

About 5% (m/v) of 50 mL aqueous extract of *R. prinoides* fruit was added to 50 mL of 3 mM $AgNO_3$ solution. The solution was allowed to react at room temperature until the color of the solution changed to red. The appearance of deep red color in the reaction vessel confirmed the formation of Ag NPs due to excitation of surface Plasmon resonance in the Ag NPs (Figure 3).

Characterization of silver nanoparticles

The synthesized Ag NPs were characterized using UV-Vis spectrometer (Agilent technologies, Cary 60UV-Vis, USA) with the wavelength range of 190 to 1100 nm. Preliminary phytochemical screening was performed to identify the different secondary metabolites present in the extract. While the FT-IR (Perkin Elmer, USA) spectroscopic analysis was performed to identify the functional groups present in the secondary metabolites and their involvement in the reduction process. The crystallinity of silver nanoparticles was examined using X-ray diffraction (PAN analytical X'Pert PRO MPD, USA) with Cu Kα radiation at a voltage of 40 KV and a current of 30 mA. The Debye–Scherrer equation was employed to calculate the average particle size of the Ag NPs.

Antibacterial assay

The antibacterial activity of the silver nanoparticle was evaluated in vitro against human pathogenic microbes, *E. coli* (Gram-negative) and *S. aureus* (Gram-positive) using the disc-diffusion method. An overnight culture of inoculum was spread over the Mueller Hinton Agar (MHA) plates by a non-toxic cotton swab on an applicator stick which was dipped into the standardized suspension of bacteria. Subsequently, the filter paper discs approximately 6 mm in diameter was soaked in a 50 µl of Ag nanoparticle colloidal solution and in a 50 µl solution of a positive control drug chloramphenicol using sterile forceps. Each disc was gently pressed down with the point of sterile forceps to ensure complete contact with the agar surface. The agar plates were then incubated at 37 ˚C for 24 hours. The plates were examined for evidence of zones of inhibition, which appear as a clear area around the wells. The diameter of such zones of inhibition was measured using a digital electronic callipers and expressed in millimetres.

RESULTS AND DISCUSSION

Preliminary phytochemical screening of aqueous extracts of *Rhamnus prinoides* fruit

Phytochemicals are plant-derived bioactive compounds. They are classified as secondary metabolites since the plants that produce them may not require them. They are produced naturally in all parts of the plant, including the leaves, stems, roots, flowers, fruits, and seeds (Ahmed et al., 2019; Hassan and Barde, 2020). Chemical tests on the aqueous extract of *R. prinoides* fruit were carried out qualitatively for the identification of various phytochemical constituents based on standard tests.

Test for Alkaloids. *R. prinoides* fruit extract was acidified by adding 1.5% (v/v) of HCl followed by a few drops of Wagner's reagent (iodine solution in potassium iodide). Formation of yellow precipitate confirms the presence of alkaloids (Bandiola, 2018; Nortjie *et al.,* 2022).

Test for Glycosides. To 1 mL of *R. prinoides* fruit extract, 1 mL of acetic acid, a drop of ferric chloride solution and then 1 mL of sulfuric acid (concentrated) were added. The formation of reddish-brown color confirmed the presence of glycosides (Gul *et at.,* 2017; Çilesizoğlu *et al.,* 2022).

Test for Tannins. About 3 mL of *R. prinoides* fruit extract was mixed with 2 mL of 0.1% of ferric chloride solution. Formation of dark brownish green color indicates the presence of tannins (Pant *et al.;* 2017; Nortjie *et al.;* 2022).

Test for Flavonoids. About 2 mL of *R. prinoides* fruit extract is mixed with 3 mL of hydrochloric acid and magnesium metal. The presence of flavonoids is confirmed by reddish coloration (Bandiola, 2018).

Test for Phenols. About 3 drops of ferric chloride solution was added to 4 mL of an aqueous *R. prinoides* fruit extract. A bluish-black color indicates the presence of phenol (Nortjie *et al.,* 2022).

Test for Carbohydrates. To 2 mL of *R. prinoides* fruit extract, 1 mL of alcoholic solution of α- naphthol is added. The mixture is shaken well and 2 mL of concentrated sulphuric acid are added slowly along the sides of the test tube. The appearance of violet ring at the junction confirmed the presence of carbohydrates (Yadav *et al*., 2017; Bandiola, 2018).

FT-IR spectral analysis

The functional groups present in the structures of the Phytochemicals present in aqueous extract of *R. prinoides* fruit that were responsible for reducing, capping, and stabilization of the Ag NPs were determined using FT-IR spectroscopic measurements. The overlaid FTIR spectra of the plant extracts and synthesized the Ag NPs is shown in Figures 3 A and B, respectively. The presence of a strong, broad band spectrum (Figure 3A) at 3459 cm^{-1} in *R. prinoides* fruit extract can be attributed to hydrogen linked O-H stretching vibrations of phenol, alcohol, carboxylic groups, and other compounds (Carmonaa *et al.,* 2017*;* Khan *et al.,* 2017*;* Masum *et al.,* 2019). At 3443 cm^{-1}, a broad absorption band for the synthesized Ag NPs was also observed (Figure 3B). This spectrum is associated with alcohol, phenolics, carboxylic groups, and other OH stretching vibrations (Pirtarighat *et al.,* 2019*;* Walelign and Legesse, 2021). A shift in the position and decrease in intensity of the Ag NPs spectrum was

observed due to O-H and N-H stretching of phenolic compounds that are present in *R. prinoides* fruit extract (Aminuzzaman *et al.*, 2018). The reason for the reduction of the intensity of the bands was due to the fact that; the phytochemicals such as alcohols, flavones, and carboxylic groups were involved in the reduction of Ag^+ to Ag nanoparticles (Kgatshe *et al.*, 2019; Khorramia *et al.*, 2019; Hemlata *et al.*, 2020). A strong absorption band for *R. prinoides* fruit extract (Figure 3A) was observed at 1638 cm^{-1}, which may be attributed to - C = C- and the $–NH_2$ of amide and amine group, mainly from proteins and enzymes (Ahmad *et al.*, 2020). The band of Ag NPs shifts to 1630 cm^{-1} with a significant reduction of its intensity. This is yet another confirmation test for the involvement of phytochemicals in the reduction process (Kgatshe *et al.*, 2019). The presence of N – H and O – H bonds in the FTIR spectrum revealed that proteins, phenolic and flavonoid compounds were responsible for the bio reduction and stabilization process of Ag NPs synthesis (Sharmila *et al.*, 2018).

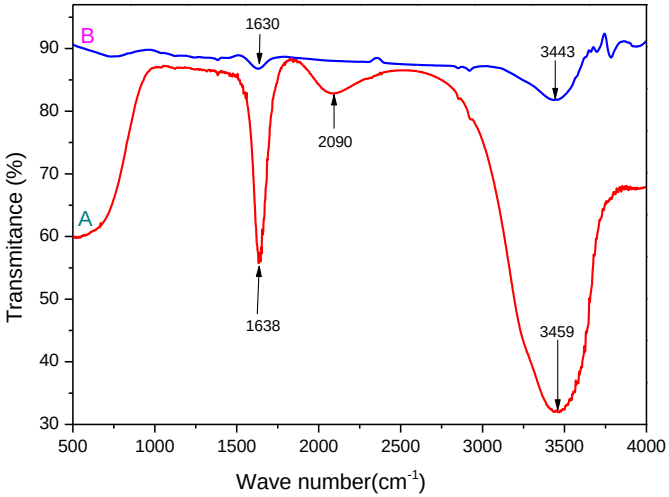

Figure 3. FTIR spectra of aqueous extract of *R. prinoides* fruit and synthesized Ag NPs.

Visual observations of formation of Ag NPs

The color change of the reaction mixture between silver nitrate solution and *R. prinoides* fruit extracts was taken as an indication of the formation of the silver nanoparticles. This was observed by color change from yellow (fruit extract) and colorless (silver nitrate) to deep red as shown in Figure 4. The appearance of deep red color in the reaction vessel indicated the formation of Ag NPs due by the reduction of the silver salt. The surface plasmon resonance, an optical property peculiar to noble

metals, was responsible for the color change (Jemal *et al.*, 2017*;* Rautela *et al.*, 2019). The reduction of silver salt to silver ions was due to the presence of reducing agents from the *R. prinoides* fruit extract (Hemlata *et al.*, 2020).

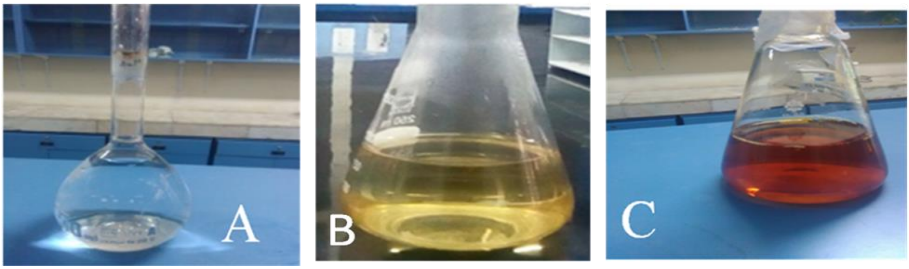

Figure 4. Color change in reaction mixture (a) Aqueous solution of silver nitrate ($AgNO_3$) (b) aqueous extract of *R. prinoides* fruit (c) Ag NPs

UV-visible spectral analysis

The UV–Visible spectra showed a distinct maximum absorbance at 416 nm which corresponds to the surface plasmon resonance of Ag NPs (Figure 5). This showed that the fruit extract has acted as a bio-reducing agent, which is consistent with the previous studies on the biosynthesis of Ag NPs from cell-free microorganism extracts and plant extracts (Aritonang *et al.*, 2019).

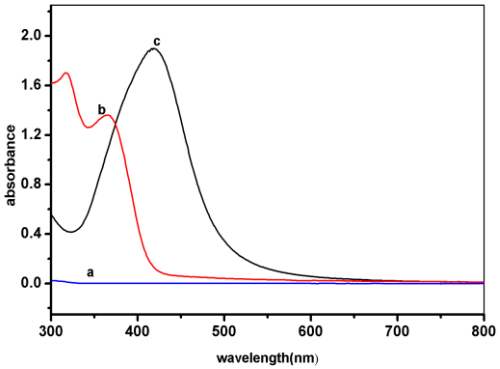

Figure 5. UV-Vis spectra of a) silver nitrate solution(blue), b) *R. prinoides* fruit extract (red) and c) Silver Nanoparticles (Ag NPs) (black).

The reduction of Ag^+ to Ag atoms by a reducing agent could account for the formation of nanoparticles. This was occurred when atoms form small clusters, which eventually expand into Ag nanoparticles (Lakshmanan *et al.*, 2018).

Optimization of parameters

Effect of silver nitrate concentration on the synthesis of Silver nanoparticles

Figure 6a shows the UV-visible spectra recorded for 50 ml of 3% (m/v) aqueous extract of *R. prinoides* fruit mixed with 50 mL of 0.5 mM, 1 mM, 1.5 mM, 2 mM, 2.5 mM, 3 mM, 4 mM of silver nitrate solution. The absorbance peak of the Ag NPs at a low concentration of AgNO3 is broad and less intense as shown in the figure. This indicates that the Ag NPs are agglomerated at lower concentrations of Ag NO3. However, as the AgNO3 concentration increases gradually from 0.5 M to 3 M, the surface plasmon resonance band becomes sharper and more intense. This indicates that as the $AgNO_3$ solution concentration rises to 3 M, the Ag NPs become significantly smaller (Ndikau *et al.,* 2017; Mukaratirwa-Muchanyereyi *et al.,* 2022). This implies that the formation of Ag NPs increased with increasing the silver nitrate concentration. As the concentration of silver nitrate solution reached at 4 mM, the intensity of the peak increases and shows little noise. Comparing the UV-Vis spectra of different Ag NO_3 concentrations, it was found that 3 mM concentration gives an intense and sharp UV-Vis spectrum. Thus, 3 mM silver nitrate solution was chosen as the optimum value.

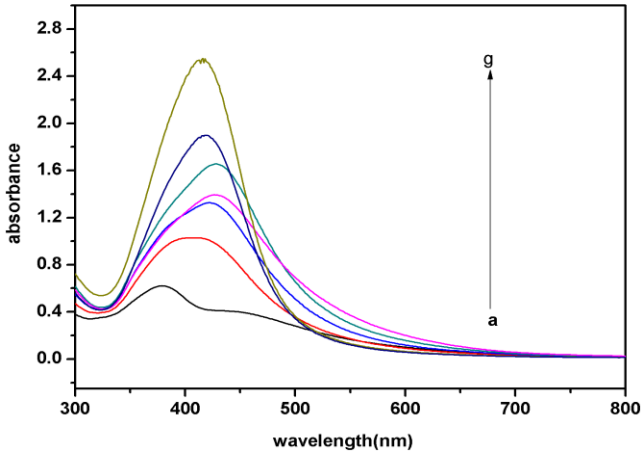

Figure 6 a. UV-Vis spectra of Ag NPs showing the effect of variation of $AgNO_3$ concentration. a) 0.5 mM b)1 mM c)1.5 mM d) 2 mM e) 2.5 mM f) 3 mM g) 4 mM

Effect of fruit extracts concentration on the synthesis of Silver nanoparticles

The effect of fruit extract concentration on the synthesis of Ag NPs was investigated using the reaction of different concentrations of *R. prinoides* fruit extract with 50 mL of 3 mM silver nitrate solution. Figure 6b shows the UV-Visible spectra of silver

nanoparticles synthesized with different concentrations of the fruit extract and a constant concentration of silver nitrate solution. At lower concentrations of the fruit extract, the UV-Visible absorbance peak was broad and less intense. But, as the fruit extract concentration increases gradually from 1% (m/v) to 6% (m/v), the absorbance peak becomes narrower and more intense. A sharp and intense absorbance peak is associated with a reduction in the size of Ag NPs. Since at lower fruit extract concentration, a smaller number of nucleation sites would be present, so more reduction would take place at one nucleus, leading to the formation of a bigger particle (Ndikau *et al*., 2017). However, at higher fruit extract concentrations, the reduction of Ag^{+} ions to Ag^{0} increases and provides a sufficient capping agent to stabilize the synthesized nanoparticles. Thus, the amount of Ag nanoparticles synthesized has increased. In this study we used 50 mL of 5% (m/v) fruit extract as the optimum value.

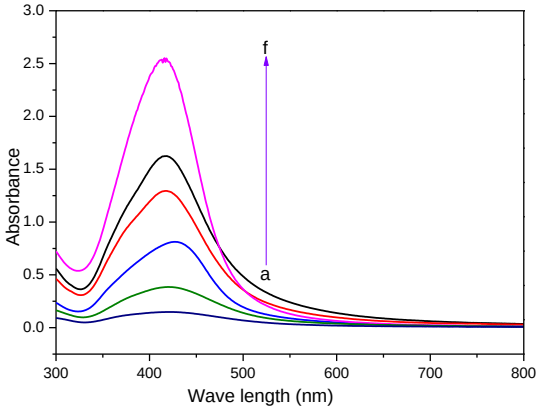

Figure 6b UV-Vis spectra of Ag NPs showing the effect of variation of *R. prinoides* amount. a)1% (m/v) b) 2% (m/v) c) 3% (m/v) d) 4% (m/v) e) 5% (m/v) f) 6% (m/v)

Effect of pH on the synthesis of Silver nanoparticles

The pH value can alter the electrical charges of biomolecules in plant extracts, affecting the nature of their capping and stabilizing affinity and, as a result, nanoparticle development (Lakshmanan *et al.*, 2018). The effect of pH on the synthesis of Ag NPs was evaluated at 1, 3, 5, 7, 9, 11, and 13 pH values. Due to Ag NP aggregation at low pH (pH 1 and 3), the UV-Vis absorption peak is considerably less intense and broad. The aggregation of Ag NPs at low pH to form large nanoparticles is favored over nucleation (Ndikau *et al.*, 2017). In acidic conditions, sluggish production and aggregation occur, resulting in bigger nanoparticles. A rise in pH usually results in a faster rate of production as well as a more uniform sized distribution of nanoparticles. When the pH of the solution was changed from acidic to the basic

solution, the NPs forms cluster distribution in the colloidal stage preventing aggregation, the absorption peak intensity increased and the spectra became intense and sharp (Patil and Chandrasekaran, 2020; Mukaratirwa-Muchanyereyi *et al.*, 2022).

At pH 13, the highest peak intensity of Ag NPs was observed. But the spectrum shows noise and becomes agglomerate at a very high pH, i.e., at pH 13, as shown in figure 6c. As a result, pH 11 was chosen as the best value for our study.

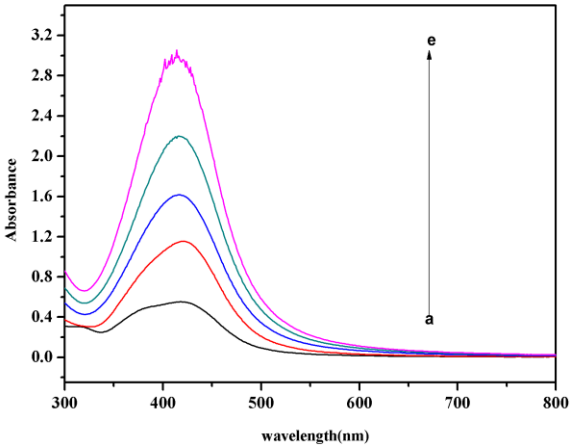

Figure 6c. UV-Vis spectra of Ag NPs showing the effect of variation of pH values a) 1, b) 3, c) 5, d) 7, e) 9, f) 11, g)13

Effect of reaction time on the synthesis of silver nanoparticles

Figure 6d shows the UV-Visible spectra of silver nanoparticles as a function of reaction time. From the figure, it is observed that the intensity of UV-Visible spectra increases as the reaction time between silver nitrate and aqueous *R. prinoides* fruit extract solution increases. This indicates that the formation of Ag NPs increased with the reaction time. At 21 hrs reaction time, the absorption peak related to the plasmon resonance of Ag NPs reached its maximum intensity, which confirmed that the biosynthesis of Ag NPs was completed. After this time, the absorption peak's strength gradually decreases, and its centre shifts to the red shift, as seen in Figure 6d (Erjaee *et al.*, 2017). Therefore, it signifies that the size of the nanoparticles grows with time, as evidenced by a redshift in the UV-Vis spectra. Hence, careful monitoring of the reaction time is required to achieve a sustainable small size of nanoparticles.

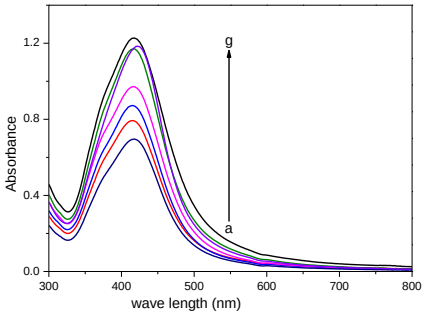

Figure 6d. UV-Vis spectra of Ag NPs showing the effect of variation of time on Ag NPs synthesis. a) 3hrs b) 6 hrs c) 9 hrs d)12 hrs e)18 hrs f)21hrs g)24 hrs

X-ray diffraction analysis

The XRD spectrum (Figure 7) revealed that the synthesized nanoparticles possessed crystalline structure (Rautela *et al.,* 2019*;* Giri *et al.,* 2022).

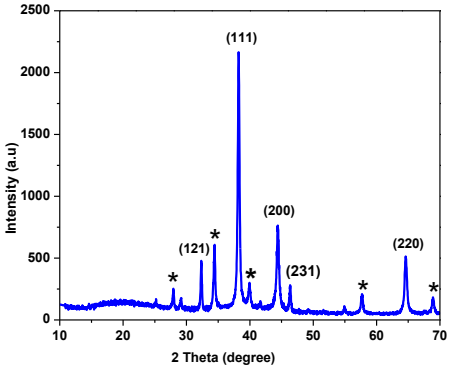

Figure 7. XRD patterns the Ag NPS.

The diffraction peaks of the nanoparticle were observed at 32.42°, 38.28°, 44.38°, 46.44° and 64.65° in the 2θ range corresponding to (121), (111), (200), (231) and (220) planes of face-centered cubic (FCC) structure of metallic silver, respectively. The Peaks observed in the patterns well agreed with the standard diffraction data with those reported for silver by joint committee on powder diffraction standards (JCPDS) File No. 04-0783 (Khan *et al.,* 2017; Dhar *et al.,* 2021; Gur, 2022; Malik *et al.,* 2022). The

particle or grain size of silver nanoparticles was determined using Debye Sherrer's equation:

$$D = \frac{0.94\lambda}{\beta \cos\theta} \quad (1)$$

Where D is the average crystalline size (A^o), λ is the x-ray wavelength (λ = 1.54 A^o), β is the full width at half maximum (FWHM) and θ is the diffraction angle.

Thus, the average particle size of Ag NPs calculated to be 21 nm. A small number of un assigned peaks (marked with stars) were also recorded that might be due to the crystallization of bioorganic phases present in the aqueous *Rhamnus prinoides* fruit extract on the surface of the silver nanoparticles (Jain *et al.,* 2017; Shaik *et al.,* 2018; Pirtarighat *et al.,* 2019). This is also another confirmatory test for the involvement of plant extracts as reducing and stabilizing agents for the synthesizing of nanoparticles.

Antibacterial activity

The antibacterial activity of the Ag NPs was examined against *E. coli* (Gram-negative), *S. aureus* (Gram-positive) bacteria using agar well-diffusion method, Figure 8.

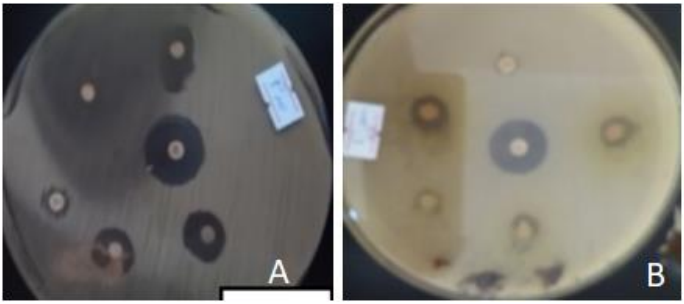

Figure 8. Disc diffusion assay of the organism a) *Escherichia coli* (Gram-negative) and b) *Staphylococcus aureus* (Gram-positive)

The antibacterial effect of the Ag NPs was determined on the basis of zone of inhibition(mm) measured by a digital electronic caliper. The maximum zone of inhibition was found against *Escherichia coli*. A medium zone of inhibition was noticed in *Staphylococcus aureus* (Table 2). According to various studies, silver nanoparticles can kill bacteria in a variety of ways. Ag nanoparticles have been demonstrated to accumulate inside the membrane and then penetrate into the cells, causing damage to cell walls or cell membranes (Jamil *et al.,* 2022). It has been

proposed that the Ag^+ ion enters the cell and intercalates between the purine and pyrimidine base pairs, breaking hydrogen bonding between the two anti-parallel strands and denaturing the DNA molecule (Walelign and Legesse, 2021).

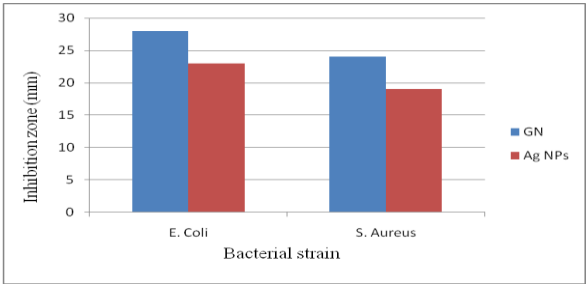

Figure 9. Comparison of antibacterial activity of Ag NPs and Gentamicin.

The general understanding is that Ag nanoparticles are typically attached to thiol groups (- SH) of enzymes, resulting in stable S - Ag interactions with thiol-containing compounds. This causes the deactivation of enzymes involved in trans membrane energy production and ion transport in the cell membrane, resulting in bacterial death (Siddiqi *et al.,* 2018). In this study, antibacterial investigations of Ag NPs exhibited significant inhibition zones against Gram positive and Gram-negative pathogens as shown in figure 9. The size of the zone of inhibitions confirmed the bactericidal efficacy of the synthesized Ag NPs against individual bacterial strains.

CONCLUSION

In this work, we used an aqueous solution of *R. prinoides* fruit extract for the synthesis of Ag NPs. The formation of a deep red color caused by surface plasmon resonance indicates the formation of Ag NPs. UV-Visible spectrophotometric, FTIR spectroscopic and X-ray diffraction measurements were used to evaluate the Ag NPs synthesized at the optimum conditions. The UV-visible absorption spectrum showed a distinct peak around 416 nm, which was a characteristic spectrum of Ag NPs. While the FTIR spectroscopic result clearly showed the involvement of the *R. prinoides* fruit extract in the reduction of Ag^+ ions to Ag NPs. The diffraction patterns were detected at 38.28˚, 44.38˚, 46.44˚, and 64.65˚ in the 2θ range, corresponding to the (111), (200), (231), and (220) planes of the face - centered cubic (FCC) structure of silver nanoparticles, respectively. The Ag NPs purity and crystallinity were confirmed by the strong and powerful characteristic peaks in the diffraction pattern. Specifically, the crystalline size of the Ag NPs was found to be 21 nm. Evaluation of the antibacterial activity of the Ag NPs gave a maximum inhibition zone of 23 mm for *E. coli* and a minimum inhibition zone of 13 nm for *S. aureus*.

ACKNOWLEDGEMENTS

The authors would like to acknowledge Department of Chemistry, Bahir Dar University, Ethiopia for the laboratory facilities.

CONFLICT OF INTEREST

The authors declare that there are no conflicts of interest for this work.

REFERENCES

Ahmad, M.A., Salmiati, S., Marpongahtun, M., Salim, M.R., Lolo, J.A and Syafiuddin, A. (2020). Green synthesis of silver nanoparticles using *Muntingia calabura* leaf extract and evaluation of antibacterial activities. *Biointerface Research in Applied Chemistry* **10**: 6253–6261.

Ahmed, M.J.I., Qin, M., Gu, P., Liu, Z., Sikandar, Y., Iqbal, A and Javeed, A.M. (2019). Phytochemical screening, total phenolic and flavonoids contents and antioxidant activities of *Citrullus colocynthis* L. and *Cannabis sativa* L. *Applied Ecology and Environmental Research* **17**: 6961–6979.

Aminuzzaman, M.,Ying, L.P., Goh, W and Watanabe, A. (2018). Green synthesis of zinc oxide nanoparticles using aqueous extract of *Garcinia mangostana* fruit pericarp and their photocatalytic activity. *Bulletin of Material Science* **41**: 1–10.

Aritonang, H.F., Koleangan, H and Wuntu, A.D. (2019). Synthesis of silver nanoparticles using aqueous extract of medicinal plants' (*Impatiens balsamina* and *Lantana camara*) fresh leaves and analysis of antimicrobial activity. *International Journal of Microbiology* **2019**: 1–9.

Arroyo, G., Angulo, Y., Debut, Aand Cumbal, L.H. (2021). Synthesis and characterization of silver nanoparticles prepared with *Carrasquilla* fruit extract (*Berberis hallii*) and evaluation of its photocatalytic activity. *Catalysts* **11**: 1–16.

Bandiola, T.M.B. (2018). Extraction and qualitative phytochemical screening of medicinal plants: a brief summary. *International Journal of Pharmacy* **8**: 137–143.

Bharadwaj, K.K., Rabha, B., Pati, S., Choudhury, B.K., Sarkar, T., Gogoi, S.K., Kakati, N. Baishya, D., Kari, Z. A and Edinur, H.A. (2021). Green synthesis of silver nanoparticles using *Diospyros malabarica* fruit extract and assessments of antimicrobial, anticancer and catalytic reduction of 4-nitrophenol (4-NP). *Nanomaterials* **11**: 1–24.

Carmonaa, E.R., Benitob, N., Plazaa, T and Recio-Sánchez, G. (2017). Green synthesis of silver nanoparticles by using leaf extracts from the endemic *Buddleja globosa* hope. *Green Chemistry Letters and Reviews* **10**: 250–256.

Çilesizoğlu, N.B., Yalçin, E., Çavuşoğlu K and Kuloğlu, S. (2022). Qualitative and quantitative phytochemical screening of *Nerium oleander* L. extracts associated with toxicity profile. *Scientific Reports* **12**: 1–16.

Devi, M., Devi, S., Sharma, V., Rana, N., Bhatia, R. K and Bhatt, A. K. (2020). Green synthesis of silver nanoparticles using methanolic fruit extract of *Aegle marmelos* and their antimicrobial potential against human bacterial pathogens. *Journal of Traditional and Complementary Medicine* **10**: 158–165.

Dhar, S.A., Chowdhury, R.A., Das, S., Nahian, M.K., Islam, D., Gafur, M.A. (2021). Plant-mediated green synthesis and characterization of silver nanoparticles using *Phyllanthus emblica* fruit extract. *Materials Today: Proceedings* **42:** 1867–1871.

Elhawary, S., EL-Hefnawy, H., Mokhtar, F.A., Sobeh, M., Mostafa, E., Osman, S and El-Raey, M. (2020). Green synthesis of silver nanoparticles using extract of *Jasminum officinale* L. leaves and evaluation of cytotoxic activity towards bladder (5637) and breast cancer (mcf-7) cell lines. *International Journal of Nanomedicine* **15:** 9771–9781.

Erjaee, H., Rajaian, H and Nazifi, S. (2017). Synthesis and characterization of novel silver nanoparticles using *Chamaemelum nobile* extract for antibacterial application. *Advances in Natural Sciences*: *Nanoscience and Nanotechnology* **8**: 1–10.

Eyob, B. (2017). Trends in production and export of gesho/*Rhamnus prinoides*/ in Ethiopia. *Research on Humanities and Social Sciences* **7**: 21–26.

Giri, A.K., Jena, B., Biswal, B., Pradhan, A.K., Arakha, M., Acharya S and Acharya, L. (2022). Green synthesis and characterization of silver nanoparticles using *Eugenia roxburghii* DC. extract and activity against bioflm-producing bacteria. *Scientifc Reports* **12**: 1–9.

Gul, R., Jan, S.U., Faridullah, S., Sherani, S and Jahan, N. (2017). Preliminary phytochemical screening, quantitative analysis of alkaloids, and antioxidant activity of crude plant extracts from *Ephedra intermedia* indigenous to Balochistan**.** *The Scientific World Journal* **2017**: 1–8.

Gur, T. (2022). Green synthesis, characterizations of silver nanoparticles using sumac (*Rhuscoriaria* L.) plant extract and their antimicrobial and DNA damage protective effects. *Frontiers in Chemistry* **10**: 1–9.

Habtemariam, A.B and Alemu, Y. (2022). Synthesis of WO3 nanoparticles using *Rhamnus prinoides* leaf extract and evaluation of its antibacterial activities. *Biointerface Research in Applied Chemistry* **12**: 529–536.

Hassan, Y and Barde, M.I. (2020). Phytochemical screening and antioxidant potential of selected Nigerian vegetables. *International Annals of Science* **8**: 12–16.

Hemalatha, K.P.J., Shantakani, S and Botcha, S. (2021). Green synthesis of silver nanoparticles using aqueous fruit and tuber extracts of *Momordica cymbalaria*. *Journal of Plant Biochemistry and Biotechnology* **3**: 196–204.

Hemlata, Meena, P.R., Singh, A.P and Tejavath, K.K. (2020). Biosynthesis of silver nanoparticles using *Cucumis prophetarum* Aqueous leaf extract and their antibacterial and antiproliferative activity against cancer cell lines. *ACS Omega* **5**: 5520–5528.

Jain, S and Mehata, M.S. (2017). Medicinal plant leaf extract and pure flavonoid mediated green synthesis of silver nanoparticles and their enhanced antibacterial property. *Scientific Reports* **7:** 1–14.

Jamil, S., Dastagir, G., Foudah, A.I., Alqarni, M.H., Yusufoglu, H.S., Alkreathy, H.M., Erturk, O., Khan, R.A and Shah, M.A. (2022). Biosynthesis of biocompatible AgNPs using medicinally important *Carduus edelbergii* Rech. f. extract for multifarious biological activities. *Journal of Nanomaterials* **2022**: 1–11.

Jemal, K., Sandeep, B.V., Pola, S. (2017). Synthesis, characterization, and evaluation of the antibacterial activity of *Allophylus serratus* leaf and leaf derived callus extracts mediated silver nanoparticles. *Journal of Nanomaterials* **2017**: 1–12.

Kgatshe, M., Aremu, O.S., Katata-Seru, L and Gopane, R. (2019). Characterization and antibacterial activity of biosynthesized silver nanoparticles using the ethanolic extract of *Pelargonium sidoides* DC. *Journal of Nanomaterials* **2019**: 1–11.

Khan, M.Z.H., Tarek, F.K., Nuzat, M., Momin, M.A and Hasan, M.R. (2017). Rapid biological synthesis of silver nanoparticles from *Ocimum sanctum* and their characterization. *Journal of Nanoscience* **2017**: 1–7.

Khorramia, S., Zarepoura, A and Zarrabi, A. (2019). Green synthesis of silver nanoparticles at low temperature in a fast pace with unique DPPH radical scavenging and selective cytotoxicity against MCF-7 and BT-20 tumor cell lines. *Biotechnology Reports* **24**: 1–8.

Lakshmanan, G., Sathiyaseelan, A., Kalaichelvan, P.T and Murugesan K.(2018). Plant-mediated synthesis of silver nanoparticles using fruit extract of *Cleome viscosa* L.: Assessment of their antibacterial and anticancer activity. *Karbala International Journal of Modern Science* **4**: 61–68.

Malik, M., Iqbal, M.A., Malik, M., Raza, M.A., Shahid, W., Choi, J.R and Pham, P.V. (2022). Biosynthesis and characterizations of silver nanoparticles from *Annona Squamosa* leaf and fruit extracts for size-dependent biomedical applications. nanomaterials **12**: 1–15.

Masum, M.M.I., Siddiqa, M.M., Ali, K.A., Zhang, Y., Abdallah, Y., Ibrahim, E., Qiu, W., Yan, C and Li, B. (2019). Biogenic synthesis of silver nanoparticles using *Phyllanthus emblica* fruit extract and its inhibitory action against the pathogen *Acidovorax oryzae* strain RS-2 of rice bacterial brown stripe. *Frontiers in Microbiology* **10**: 1–18.

Moond, M., Singh, S., Sangwan, S., Devi, R and Beniwal, R. (2022). Green synthesis and applications of silver nanoparticles: A systematic review. *AATCC Journal of Research* **9**: 272 –285.

Mukaratirwa-Muchanyereyi, N., Gusha, C., Mujuru, M., Guyo, U and Nyoni, S. (2022). Synthesis of silver nanoparticles using plant extracts from *Erythrina abyssinica* aerial parts and assessment of their anti-bacterial and anti-oxidant activities. *Results in Chemistry* **4**: 1–7.

Negash, A.W., Tadesse, B.T and Tsehai, B.A. (2021).Assessment and determination of bittering agents, essential oils, and antioxidants of gesho (*Rhamnus prinoides* L. Herit) collected from Amhara Region, Ethiopia. *Journal of Chemistry* **2021**: 1–7.

Ndikau, M., Noah, N.M., Andala, D.M and Masika, E. (2017). Green synthesis and characterization of silver nanoparticles using *Citrullus lanatus* fruit rind extract. *International Journal of Analytical Chemistry* **2017**: 1–10.

Niluxsshun, M.C.D., Masilamani, K and Mathiventhan, U. (2021). Green synthesis of silver nanoparticles from the extracts of fruit peel of *Citrus tangerina*, *Citrus sinensis*, and *Citrus limon* for antibacterial activities. *Bioinorganic Chemistry and Applications* **2017**: 1–8.

Nortjie, E., Basitere, M., Moyo, D and Nyamukamba, P. (2022). Extraction methods, quantitative and qualitative phytochemical screening of medicinal plants for antimicrobial textiles: A review. *Plants* **11**: 1–17.

Pant, D.R., Pant, N.D., Saru, D.B., Yadav, U.N and Khanal, D.P. (2017). Phytochemical screening and study of antioxidant, antimicrobial, antidiabetic, anti-inflammatory and analgesic activities of extracts from stem wood of *Pterocarpus marsupium* Roxburgh. *Journal of Intercultural Ethnopharmacology* **6**: 170–176.

Patil, S and Chandrasekaran, R. (2020). Biogenic nanoparticles: a comprehensive perspective in synthesis, characterization, application and its challenges. *Journal of Genetic Engineering and Biotechnology* **18**: 1–23.

Pirtarighat, S., Ghannadnia, M and Baghshahi, S. (2019). Green synthesis of silver nanoparticles using the plant extract of *Salvia spinosa* grown in vitro and their antibacterial activity assessment. *Journal of Nanostructure in Chemistry* **9**: 1–9.

Rautela, A., Rani, J and Debnath (Das), M. (2019). Green synthesis of silver nanoparticles from *Tectona grandis* seeds extract: Characterization and mechanism of antimicrobial action on different microorganisms. *Journal of Analytical Science and Technology* **10**: 1–10.

Saidu, F.K., Mathew, A., Parveen, A., Valiyathra,V and Thomas G.V. (2019). Novel green synthesis of silver nanoparticles using clammy cherry (*Cordia obliqua* Willd) fruit extract and investigation on its catalytic and antimicrobial properties. *SN Applied Sciences* **1**: 1–13.

Shaik, M.R., Khan, M., Kuniyil, M., Al-Warthan, A., Alkhathlan, H.Z., Siddiqui, M.R.H., Shaik, J.P., Ahamed, A., Mahmood, Khan, A.M and Adil, S.F. (2018). Plant-extract-assisted green synthesis of silver nanoparticles using *Origanum vulgare* L. extract and their microbicidal activities. *Sustainability* **10**: 1–14.

Sharmila, G., Muthukumaran, C., Sandiya, K., Santhiya, S., Pradeep, R.S., Manoj, N., Suriyanarayanan, K.N and Thirumarimurugan, M. (2018). Biosynthesis, characterization, and antibacterial activity of zinc oxide nanoparticles derived from *Bauhinia tomentosa* leaf extract. *Journal of Nanostructure in Chemistry* **8**: 1–7.

Siddiqi, K.S., Husen, A and Rao, R.A.K. (2018). A review on biosynthesis of silver nanoparticles and their biocidal properties. *Journal of Nanobiotechnology* **16**: 1–28.

Vanlalveni, C., Lallianrawna, S., Biswas, A., Selvaraj, M., Changmai, B and Rokhum, S.L. (2021). Green synthesis of silver nanoparticles using plant extracts and their antimicrobial activities: a review of recent literature. *RSC Advances* **11**: 2804–2837.

Walelign, W and Legesse, T. (2021). Green synthesis of silver nanoparticles using *Hagenia abyssinica* (Bruce) J.F. Gmel plant leaf extract and their antibacterial and anti-oxidant activities. *Heliyon* **7**: 1–11.

Yadav, R., Khare, R.K and Singhal, A. (2017). Qualitative phytochemical screening of some selected medicinal plants of Shivpuri District. *International Journal of Life Sciences and Scientific Research* **3**: 844–847.